Modulation of locus coeruleus neurons and strong release of noradrenaline during acute hippocampal seizures in rats

Lars Emil Larsen[*1,2], Sielke Caestecker[*1], Latoya Stevens[3], Pieter van Mierlo[2], Evelien Carrette[1], Paul Boon[1], Kristl Vonck[1], Robrecht Raedt[1]

[*]Shared-first author, these authors contributed equally

[1] 4BRAIN, Department of Head and Skin, Ghent University, Ghent, Belgium

[2] Medical Image and Signal Processing, Department of Electronics and Information Systems, Ghent University, Ghent, Belgium

[3] Vrije Universiteit Brussel (VUB), Universitair Ziekenhuis Brussel (UZ Brussel), Department of Medical Oncology/Laboratory for Molecular and Medical Oncology (LMMO), Brussels Belgium.

Abstract

The locus coeruleus (LC), a brainstem nucleus, is the sole source of noradrenaline in the neocortex, hippocampus and cerebellum. Noradrenaline is a powerful neuromodulator involved in the regulation of excitability and plasticity of large-scale brain networks. In this study, we assessed the activity of locus coeruleus neurons and changes in noradrenergic transmission during acute hippocampal seizures evoked with perforant path stimulation. LC neurons were recorded in anesthetized rats using a multichannel electrophysiology probe and were identified based on electrophysiological characteristics or optogenetic tagging. The majority of LC neurons (55%) were inhibited during seizures, while only a subset of LC neurons (28%) was excited during seizures. Topographic analysis of multi-unit activity showed anatomical separation of neurons that were excited and inhibited during seizures. Changes in hippocampal noradrenaline transmission during seizures were assessed using a fluorescent biosensor for noradrenaline, $GRAB_{NE2m}$, in combination with fiber photometry in both anesthetized and awake rats. Our results indicate that acute electrically evoked hippocampal seizures are associated with strong changes in LC unit activity and strong and consistent time-locked release of noradrenaline. Understanding the role of mass release of noradrenaline during hippocampal seizures is likely to be important to understand seizure pathophysiology.

Introduction

The locus coeruleus (LC) consists of a small cluster of noradrenergic neurons in the brainstem. Through widespread axonal connections, the LC is the main source of noradrenaline for most brain structures, including the neocortex and hippocampus (Benarroch, 2018). Release of noradrenaline in the target structures is known to modulate a number of physiological processes including arousal, attention, memory and emotional processing and exerts powerful control over circuit excitability and plasticity (Berridge & Waterhouse, 2003; Harley, 2007; Sara, 2009). In the context of epilepsy, noradrenaline is generally considered an anticonvulsant neuromodulator (Ghasemi & Mehranfard, 2018). Lesions to the LC-noradrenergic system are known to result in severe exacerbation of seizures in rodent epilepsy models (McIntyre et al., 1979; Mishira et al., 1994). Meanwhile, although less consistent, therapeutic interventions elevating noradrenergic transmission are often observed to reduce the severity of seizures (Clinckers et al., 2010; Raedt et al., 2011; Vermoesen et al., 2012). Other studies, however, have claimed proconvulsant effects of noradrenaline under certain conditions, which has been attributed to activation of different subtypes of adrenoceptors of the α- and β-families (Ghasemi & Mehranfard, 2018). The diversity of adrenoceptors throughout various brain areas and in diverse cell populations, including neuronal (Berridge & Waterhouse, 2003) and glial cell populations (Batiuk et al., 2020), may explain the multitude of effects observed. Next to that, the difference in affinity between the different adrenoceptor subtypes, could point towards concentration-dependent effects, depending on a gradual but step-wise recruitment of respectively α_2-, α_1- and β-adrenoceptors (Atzori et al., 2016).

Beyond seizure modulating properties of noradrenaline, there is also evidence that the LC-noradrenergic system may play a more direct role in epileptic disorders. There are indications that the transitioning from a healthy to an epileptic brain following a status epilepticus, also known as epileptogenesis, results in changes in expression patterns of adrenoceptors throughout the brain, which may result in a net decrease in the efficiency of noradrenergic transmission (Corcoran & Weiss, 1990a). Evidence also indicates that the LC-noradrenergic system is activated during chemically and electrically evoked seizures in rodents (Jimenez-

53 Rivera & Weiss, 1989; Silveira et al., 2000, 2002; Silveira, Liu, de LaCalle, et al., 1998; Silveira, Liu, Holmes, et
54 al., 1998). Limbic seizures have been associated with increased expression of cFos, a marker for neuronal
55 activation, in LC neurons (Silveira et al., 2000, 2002; Silveira, Liu, de LaCalle, et al., 1998; Silveira, Liu, Holmes,
56 et al., 1998), while a previous report suggests an increase in LC multiunit activity in seizures evoked by
57 electrical stimulation of the amygdala (Jimenez-Rivera & Weiss, 1989). This suggests that understanding how
58 the LC-noradrenergic system is affected by seizures can be key to understanding seizure pathophysiology.

59 In this study, we investigated changes in LC-unit activity and LC-noradrenergic transmission during acute
60 hippocampal seizures in rodents applying novel neuroscientific research tools such as high-density
61 electrophysiology, optogenetics and noradrenaline biosensing. The identity of LC neurons was additionally
62 confirmed through optogenetic tagging, where LC specific expression of the inhibitory opsin GtACR2 was
63 combined with blue light illumination, allowing LC neuron identification *in vivo* (Lee et al., 2020; Lima et al.,
64 2009). The recently developed $GRAB_{NE2m}$ biosensor (Feng et al., 2019) was used to assess changes in
65 noradrenergic transmission in the hippocampus during seizures with high subsecond temporal precision.

66 # Results

67 **Characteristics of evoked hippocampal seizures**

68 Hippocampal seizures were evoked in anesthetized male Sprague Dawley rats with 10s tetanic trains of
69 perforant path stimulation (20 Hz, 0.2 ms bipolar square wave pulses), using stimulation intensities ranging
70 from 300-800 µA. The seizures were initially characterized by repetitive high-amplitude negative spikes in
71 the local field and a general increase in broad band power (**Figure 1** and **supplementary Figure 1**). Seizure
72 duration was very stable within animals when evoking multiple seizures, but was observed to vary between
73 animals. The mean duration of the first seizure evoked in each experimental session across all animals was
74 13.1±4.8 seconds (mean ± SD; range 5.3-24.0 seconds).

75 **Evoked hippocampal seizures modulate the firing of locus coeruleus neurons**

76 LC neurons were targeted using three different electrode set-ups: 1) a single-channel tungsten
77 microelectrode, 2) a 32-channel silicon probe and 3) a 32-channel silicon probe with a Ø100 µm optical fiber
78 attached, terminating at the most proximal electrode contact.

79 Single channel recordings yielded a total of 8 clusters of neurons recorded in 5 out of 9 animals. Spike sorting
80 based on the single channel recordings did not always allow unambiguous characterization of single-unit
81 activity, for which the putative LC neurons isolated in the single channel LC recordings are referred to as 'LC
82 neuron clusters' and may in some cases reflect multiple neurons. All identified neuron clusters responded
83 with a typical burst-inhibition to noxious stimuli and were inhibited following administration of
84 clonidine (0.04 mg/kg, I.P.), an agonist of the α_2-adrenergic receptor, upon conclusion of the experiments.
85 Evoked hippocampal seizures were associated with profound changes in firing rate of most of the recorded
86 LC neuron clusters, although both increased and decreased firing was observed (**Figure 1**). The first evoked
87 hippocampal seizure resulted in increased firing in five LC neuron clusters, while one LC neuron cluster was
88 significantly inhibited during seizures. Two LC neuron clusters showed no significant changes in firing during
89 seizures. The response of LC neuron clusters was observed to be consistent over consecutively evoked

90 seizures. Additional LC recordings were performed using high-density silicon probes to increase the yield of
91 neurons recorded and the validity of the spike sorting process.

92 Using a 32-channel high-density electrophysiology probe, LC activity was identified in 9 out of 14 animals. In
93 two animals, recordings were performed both ipsilateral and contralateral to the side of the perforant path
94 stimulation. In total, recordings resulted in the identification of 97 LC neurons that responded to noxious foot
95 pinches or were tagged using optogenetics with LC-specific expression of the inhibitory opsin GtACR2 (**Figure**
96 **8**, **supplementary Figure 2**). Identified neurons further responded with pronounced inhibition following
97 administration of clonidine (0.04 mg/kg, I.P.). Before and between seizures, the mean firing rate of recorded
98 neurons was 2.3 Hz ± 1.4 Hz (median 2.1 Hz). In contrast to the single-channel recordings, a majority of
99 neurons recorded, 54 (56%), were significantly inhibited during seizures. Only 27 (28%) LC neurons were
100 excited during seizures, while a minority of 16 (16%) LC neurons showed no significant change in firing rate.
101 Changes in LC firing were typically aligned with the onset of hippocampal seizure activity. The response of
102 individual neurons was observed to be consistent over subsequently evoked seizures, with 59% and 62% of
103 LC neurons being inhibited and 25% and 22% of LC neurons being excited during the second and third seizure,
104 respectively. The responses of individual LC neurons over consecutively evoked seizures were highly
105 correlated (r=0.87, 0.80 and 0.92 for seizure 1 vs. seizure 2, seizure 1 vs. seizure 3 and seizure 2 vs. seizure 3,
106 respectively, **supplementary Figure 3**).

107 Around 35% of the 97 neurons recorded from the LC, were recorded contralateral to the stimulated perforant
108 path. However, the fraction of neurons responding with excitation vs. inhibition in relation to the evoked
109 seizure for contralateral (44%/52%) vs. ipsilateral (32%/56%) recordings was not found to substantially differ.

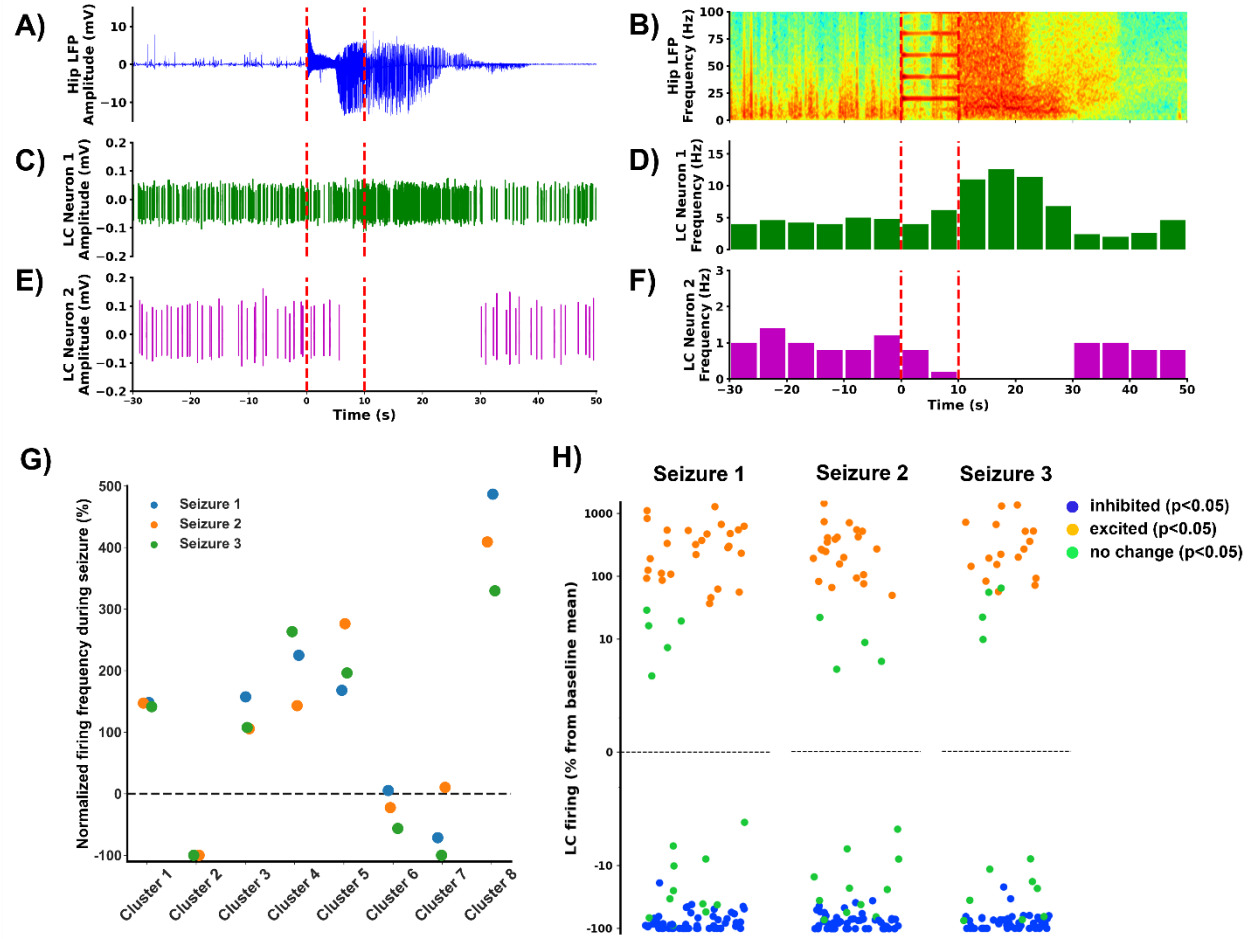

Figure 1: Example of an electrically evoked hippocampal seizure and associated changes in firing rates of locus coeruleus (LC) neurons. Hippocampal seizures were induced with 10s tetanic burst stimuli delivered in the perforant path, denoted with red dashed lines. A) Hippocampal local field potential (LFP) trace, B) a spectrogram of the hippocampal LFP, C) and D) example of LC neurons displaying increased firing during hippocampal seizures, E) and F) example of a LC neurons showing decreased firing during hippocampal seizures, G) normalized changes in firing rates of the LC neurons identified based on single channel tungsten needle recordings and H) normalized changes in firing rates of neurons identified from multi-channel probe recordings. In G) and H), firing rates during hippocampal seizures have been normalized to the mean firing rate the minute before seizure induction.

Characteristics of inhibited versus excited locus coeruleus neurons

Next, we aimed to identify potentially separating characteristics of inhibited vs. excited LC neurons. Previous studies have indeed suggested the presence of distinct types of LC neurons that can be distinguished on the basis of spike waveforms and spike rate (Totah et al., 2018a). Our data, however, did not show any tendencies for such clustering (**supplementary Figure 4A-C**). Next we assessed whether spike width, peak asymmetry in

spike waveforms, mean spike rate or median interspike interval could predict the response of LC neurons to evoked hippocampal seizures. However, no such relationship was indicated by our analyses (**supplementary Figure 4D-G**).

Additionally, the type of coupling between LC neurons, broad (tens of milliseconds) or sharp (< millisecond) coupling, was assessed to investigate a possible correlation to the excitatory or inhibitory activity during an evoked hippocampal seizure (Totah et al., 2018). Both types of coupling were observed in our data, when looking at the spontaneous spiking patterns of neurons in the absence of seizures, and at rates comparable to those observed in literature (**supplementary Figure 5**). However, the rates of significant cross-correlograms were similar for pairs of inhibited neurons, pairs of excited neurons and pairs of inhibited and excited neurons (**supplementary Figure 5E**). Finally, we evaluated cross-correlation between neurons that were excited during seizures (58 neuron pairs). A limited number of spikes was measured due to a limiting sampling period (50-seconds around the seizures, 2-3 seizures per recording). The fraction of correlated neurons during seizures was similar to the fraction during interictal periods. Although not all neuron pairs with interictal coupling showed coupling during seizures, preictal sharp coupling was nevertheless observed to predict coupling during seizures ($p<0.05$, Fisher's exact test).

In a final attempt to understand potential differences between neurons inhibited or excited in relation to seizures, we focused on anatomy. The high-density multi-channel probe enabled us to compute topographies of the changes in multiunit-activity across the probe in relation to seizures or other events. Beyond confirming the presence of both inhibited and excited LC neurons in relation to seizures, such analysis additionally indicated anatomical separation of clusters of neurons responding to seizures with inhibition vs. excitation (**Figure 2**). Although with some degree of variability, such pattern was observed in multiple animals (**supplementary Figure 6**) and was observed to be highly consistent over the course of multiple, consecutively evoked hippocampal seizures (**Figure 2**).

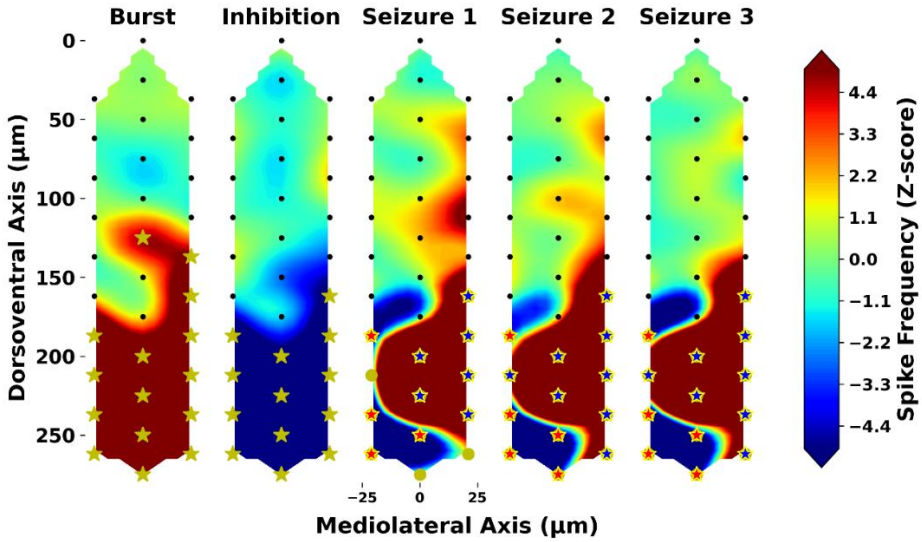

Figure 2: A filled contour plot to illustrate multiunit firing rates across the 32-channel recording probe in relation to specific events. Firing rates have been geometrically interpolated by means of cubic interpolation. Left, in the first two plots, is an illustration of the average noxious foot pinch response characterized by a burst, subsequently followed by inhibition. Significant responses at an individual channel level are indicated with yellow stars. The example provided shows profound and very consistent changes in multiunit activity across the probe in relation to repeated seizure inductions. Significant inhibition is noted with red stars and significant excitation is noted with blue stars. Channels marked as LC channels based on significant burst inhibition in response to a noxious foot pinch are additionally noted with a yellow edge around the stars.

Coupling of LC neurons to the hippocampal LFP during evoked hippocampal seizures

From initial observations it was clear that changes in LC activity coincided with the occurrence of seizure activity in the hippocampal LFP. In a few cases, intermittent seizure activity in the hippocampal field was even associated with additional bursts of activity in these neurons (**supplementary Figure 9**). A quantitative analysis of this temporal association was performed by means of cross-correlation of 1-second hippocampal LFP amplitude bins and LC neuron spike rate bins (**Figure 3**). Since it was difficult to analyze the hippocampal LFP reliably during seizure induction, due to electrical stimulation artefacts and difficulties dissociating evoked field activity from seizure activity, analysis focused on the 50 seconds immediately following stimulation and thus in particular the timing of seizure termination and normalization of LC firing (**Figure 3A**). Analysis revealed neurons displaying strong anticorrelation and correlation to the amplitude of the hippocampal LFP, reflecting LC neurons showing inhibition and excitation in relation to seizures, respectively.

166 Few neurons showed no clear correlation with the hippocampal LFP (**Figure 3B**). A density-based clustering
167 analysis on the basis of peak cross-correlation and lag indeed allowed the identification of two clear clusters
168 of neurons showing strong anticorrelation (n = 51 neurons) and correlation (n = 25 neurons) to the amplitude
169 of the hippocampal LFP (**Figure 3C**). While there was no detectable difference in the lag of their association,
170 neurons excited by seizures displayed a stronger peak cross-correlation with the amplitude of the
171 hippocampal LFP than inhibited neurons (0.85±0.11 vs. 0.78±0.09, p<0.001). In the vast majority of cases,
172 peak correlation was observed with a negative lag or at 0, indicating that firing of LC neurons normalized
173 before normalization in hippocampal LFP amplitude.

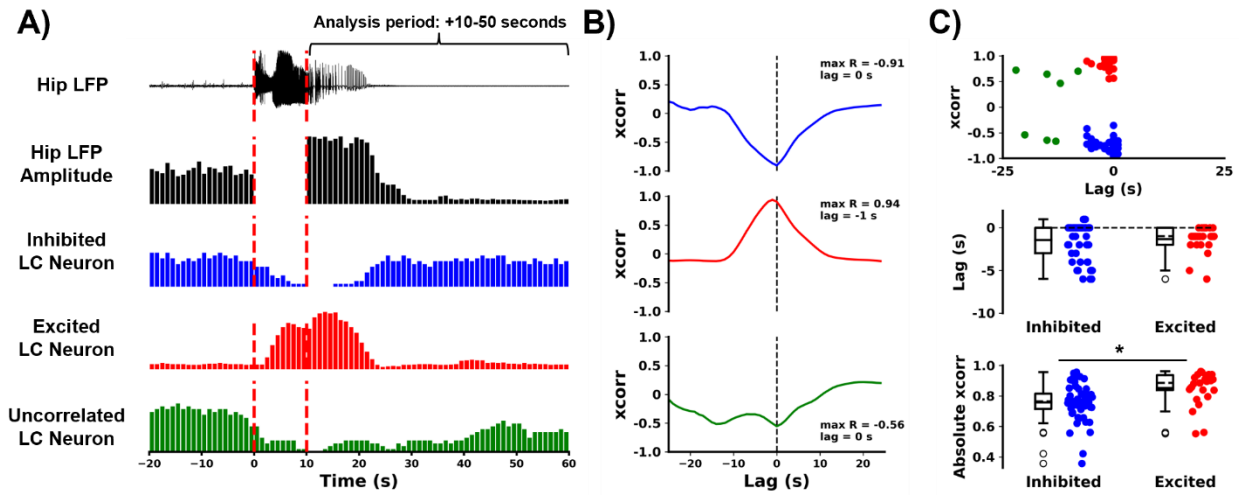

174 **Figure 3:** Temporal association between seizure activity in the hippocampal local field potential (LFP) and changes in
175 the firing of locus coeruleus (LC) neurons. A) Cross-correlation analyses were based on 1 second bins of hippocampal
176 LFP amplitude and firing rates of individual LC neurons. B) Cross-correlation (xcorr) analysis revealed the presence of LC
177 neurons showing strong anticorrelation to changes in hippocampal LFP amplitude (inhibited neurons), neurons showing
178 strong direct correlation (excited neurons) and neurons showing weak correlation (uncorrelated neurons) to the
179 50 seconds immediately following electrical seizure induction. C) Anticorrelated and directly correlated LC neurons
180 could be separated with a density-based clustering analysis which showed similar lag, but a strong cross-correlation of
181 excited vs. inhibited neurons (* denoting statistical significance).

182 A few excited neurons were additionally observed to display coupling to the phase of the hippocampal LFP (8-
183 16 Hz), which exceeded what could be expected by chance even after Bonferroni correction (**Figure 4**). None
184 of these neurons showed any corresponding coupling to the phase of the hippocampal LFP in the 60 seconds
185 prior to seizure induction (**supplementary Figure 9**). Three of the five neurons displaying significant phase

coupling to the hippocampal seizure LFP were identified in the same recording and were observed to generally bind to the throughs of the filtered 8-16 Hz hippocampal LFP signal. During a second seizure, only one of the three neurons retained significant coupling to the hippocampal seizure LFP ($p<0.01$), while coupling of a second neuron was trending towards significance following Bonferroni correction ($p=0.085$) (**supplementary Figure 8**).

An additional analysis assessed coupling between spiking of LC neurons and the occurrence of spikes in the hippocampal LFP in relation to the seizures (**supplementary Figure 9**). While two neurons showed statistically significant increased likelihood of spiking around the time of hippocampal LFP spikes, the relationship did not remain following Bonferroni correction for multiple testing.

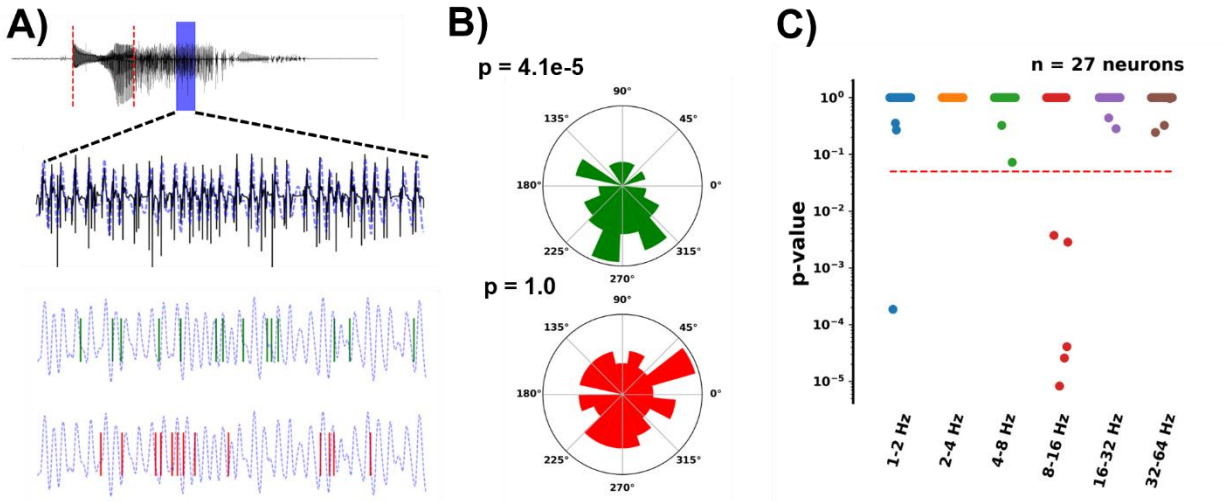

Figure 4: Phase preference of locus coeruleus (LC) neurons to the hippocampal local field potential (LFP) during evoked seizures. A) Example of hippocampal LFP, which was filtered in varying frequency bands (blue dashed lines) and B) example of an LC neuron displaying significant phase preference to the 8-16 Hz bandpass filtered hippocampal LFP (green) and an uncoupled neuron (red). C) An overview of all neurons following significance correction, showing that 5 LC neurons displayed significant coupling to the hippocampal 8-16 Hz LFP.

Photometric quantification of $GRAB_{NE2m}$ in relation to hippocampal seizures

Beyond assessing changes in LC unit activity, a fluorescent sensor for noradrenaline, $GRAB_{NE2m}$, was used to quantify changes in noradrenaline release in the hippocampus in relation to evoked hippocampal seizures (**Figure 5**). Induction of hippocampal seizures was observed to consistently increase $GRAB_{NE2m}$

205 fluorescence both in anesthetized (31.5 ± 33.8%) as well as awake (23.9 ± 16.2%) conditions, indicating an
206 increase in extracellular noradrenaline concentration. While the extent of the change in $GRAB_{NE2m}$
207 fluorescence was highly variable at a group level (range anaesthesia: 5.6 - 107.1%, range awake: 6.9 – 60.1%,
208 **Figure 5D and H**), the peak changes observed were nevertheless consistently far beyond what could be
209 expected by chance for individual animals (z-score range anaesthesia: 6.8 – 502.2, z-score range
210 awake: 16.0 - 380.6, **Figure 5E and I**). Similar to previous observations of temporal correlations between
211 changes in hippocampal LFP amplitude and LC unit activity, a strong correlation was observed between
212 changes in $GRAB_{NE2m}$ fluorescence and hippocampal LFP amplitude in relation to seizures. Negative lags
213 indicate a tendency for the GRAB-signal to peak prior to normalization of the hippocampal LFP.

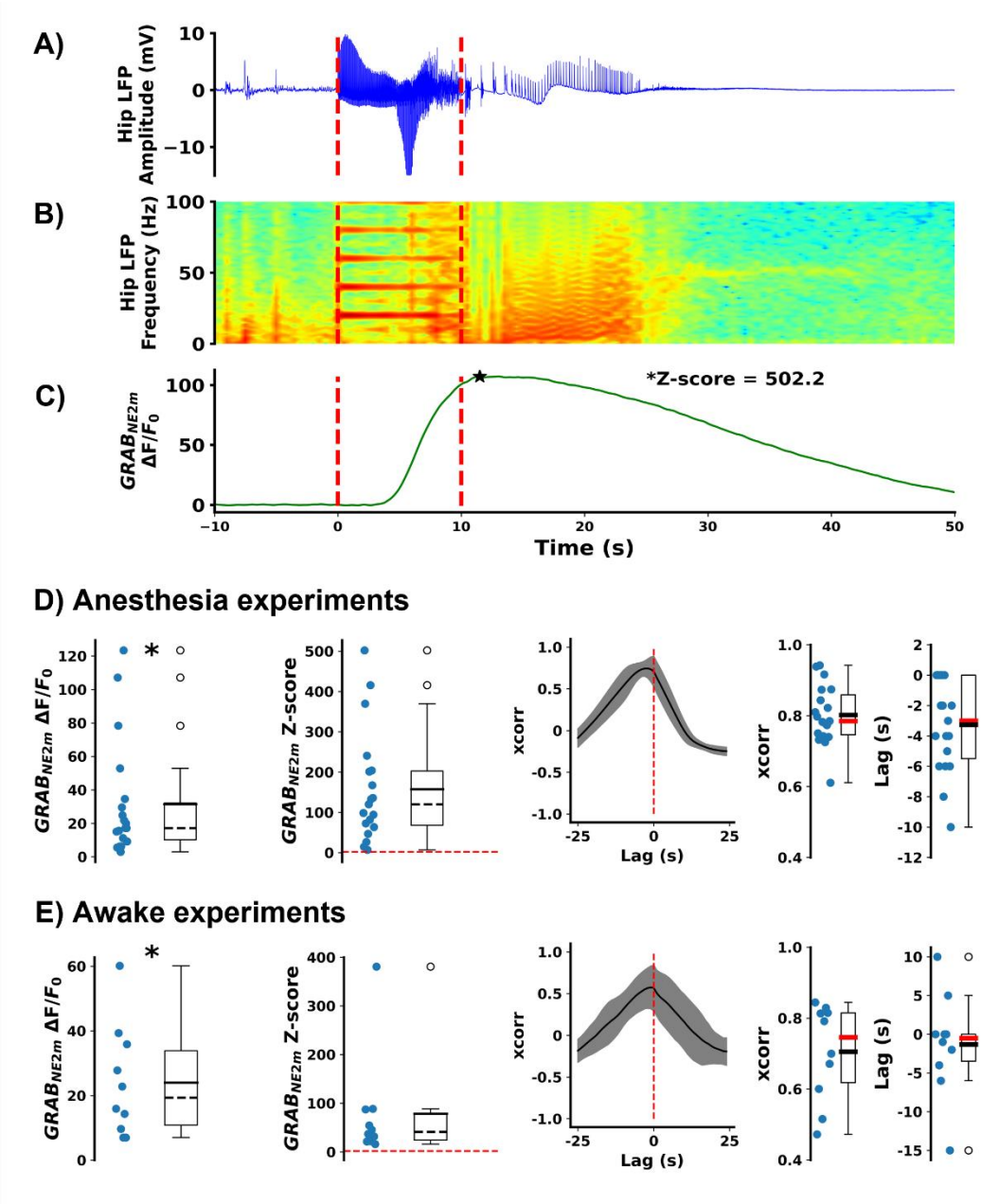

Figure 5: Changes in noradrenergic transmission in the hippocampus were assessed using the fluorescent sensor for noradrenaline $GRAB_{NE2m}$ in combination with fiber photometry. A-C) Perforant path stimulation induced seizures (red dashed lines) were associated with an increase in $GRAB_{NE2m}$ fluorescence. Similar outcomes were observed in anesthetized (D) and awake rats (E), * indicates the peak response in fluorescence for one animal after a seizure. Changes were observed to be highly significant both at a group level and individual level. Changes in $GRAB_{NE2m}$ fluorescence were further found to be correlated to changes in hippocampal LFP amplitude when cross correlating 1-second amplitude bins over the 50-second period following electrical stimulation.

Discussion

Previous studies have indicated that various types of seizures in rodent seizure models modulate the LC-noradrenergic system (Jimenez-Rivera & Weiss, 1989; Silveira et al., 2000, 2002; Silveira, Liu, de LaCalle, et al., 1998; Silveira, Liu, Holmes, et al., 1998). In this study, we used a 32-channel high-density probe for LC unit recording and the recently developed $GRAB_{NE2m}$ biosensor for noradrenaline detection, to perform a detailed assessment of the effect of evoked hippocampal seizures on LC-noradrenergic transmission. We found that hippocampal seizures consistently modulated LC activity and led to a strong release of noradrenaline in the hippocampus. Understanding the physiological or pathophysiological implications of this release is likely to be important to understanding the pathophysiology of seizures.

In a series of initial single channel recordings of LC unit activity with tungsten electrodes, we recorded few neuron clusters of which a majority showed increased firing during seizures (5/8), which thus aligned with our initial expectations (Jimenez-Rivera & Weiss, 1989; Silveira, Liu, de LaCalle, et al., 1998; Silveira, Liu, Holmes, et al., 1998). Subsequent high-density recordings using 32-channel silicon probes, yielded a higher number of LC neurons (97). However, here, most neurons (~55%) were inhibited in relation to seizures, while only a small subset of neurons (~25%) increased their firing. The responses of neurons were consistent over consecutively evoked seizures. Interestingly, literature does indeed indicate distinct classes of LC neurons (Totah et al., 2018). In particular, evidence suggests the presence of slow spiking LC neurons with broad waveforms located predominantly in the dorsal LC, while the ventral LC contains neurons characterized by faster spike rates and narrow waveforms (Totah et al., 2018). Our data, however, did not show any clear clusters of neurons based on spike wave forms and firing rate, but showed the presence of one rather uniform cluster with a mean firing rate of around 2 Hz, which is on the high side relative to typical reports in literature. One explanation, although we have no conclusive evidence hereof, is that we likely recorded mainly from the dorsal LC, as recordings were usually initiated upon the first encounter of LC activity, without lowering the electrode or probe further with the risk of losing LC activity. Here, it is also important to note that LC

247 recordings were conducted using state-of-the-art methodology, including optogenetic tagging of LC activity,
248 resulting in a high level of confidence that LC neuronal activity was being recorded.

249 The lack of distinct classes of LC neurons in our data further meant that any attempts to separate or
250 characterize inhibited and excited LC neurons on the basis of the baseline firing frequency or waveforms, did
251 not show any meaningful correlations. Instead, we calculated cross-correlation of neurons, which has been
252 described to a limited extent in literature and which is thought to reflect either common synaptic inputs
253 (coupling over tens or hundreds of milliseconds) or electrotonic coupling via gap junctions (coupling within a
254 millisecond) (Totah et al., 2018). Indeed, we observed both types of coupling in our data, and at rates
255 comparable to previous reports (Breton-Provencher et al., 2021). However, although we initially
256 hypothesized a higher rate of coupling among excited neuron pairs as a potential explanation for common
257 excitatory drive, this did not appear to be the case in our data.

258 Thus, in a final attempt to comprehend possible differences between neurons that respond differently to
259 seizures, we computed topographies of multi-unit activity across the 32-channel probes used for recordings.
260 In this case in at least half of the recordings (5/9), anatomical separation of inhibited vs. excited activity was
261 observed. Interestingly, and contrary to early evidence (Berridge & Waterhouse, 2003), more recent studies
262 suggest that the LC is not a single uniform unit, but that LC neurons are arranged in anatomically distinct
263 modules in accordance with their efferent projection patterns (Chandler et al., 2019; Uematsu et al., 2017).
264 Considering that we consistently observed an increase in noradrenergic transmission in the hippocampus, as
265 shown in the $GRAB_{NE2m}$ experiments, at least part of the neurons excited in relation to hippocampal seizures
266 must be neurons projecting to the hippocampal formation. A definite proof hereof, however, would require
267 either antidromic tagging or the use of e.g. retrogradely transduced opsins (Li et al., 2016). Secondly, it must
268 be considered that a majority of LC neurons (56%) recorded were still inhibited during seizures. With the
269 proposed modular arrangement of the LC in mind (Chandler et al., 2019; Uematsu et al., 2017), it is therefore
270 likely that inhibited neurons innervate other targets than the hippocampal formation, which therefore may

271 result in a drop in noradrenaline concentrations in other parts of the central nervous system in relation to
272 seizures.

273 Exactly how evoked hippocampal seizures result in modulation of LC neurons, and strong release of
274 hippocampal noradrenaline, remains unclear. Considering that seizures were evoked by electrical stimulation
275 of the perforant path, which is located externally to the hippocampus, it is unlikely that LC projections were
276 stimulated directly and activated antidromically. Changes in LC firing were further aligned with the onset of
277 seizure activity in the hippocampus, which typically had a 5-7 second latency from the onset of the electrical
278 stimulation, further countering this argument. Although the LC provides noradrenergic innervation to the
279 hippocampus (Mason & Fibiger, 1979), there are no known direct projections from the hippocampus to the
280 LC (Sara & Bouret, 2012). Rather, pathways to the LC from the hippocampal formation are polysynaptic
281 connections, such as those via the amygdala or the prefrontal cortex (Breton-Provencher et al., 2021).
282 Afferent projections from the prefrontal cortex to the LC are ionotropic glutamatergic connections, while
283 projections from the amygdala release corticotropin releasing hormone (CRH), which induces excitation
284 through activation of G-protein coupled receptors (Breton-Provencher et al., 2021). This motivated a closer
285 look at potential correlations between the hippocampal local field potential and LC unit activity in relation to
286 seizures. Here, it was clear that changes in LC activity in most cases were confined specifically to the period
287 of the evoked hippocampal seizure. The fast onset and normalization of LC activity following termination of
288 seizure activity would not suggest the involvement of metabotropic receptors which usually would have slow
289 but long-lasting effects. Rather, the data suggests a strong excitatory input to LC neurons excited by
290 hippocampal seizures via a yet undefined ionotropic glutamatergic polysynaptic pathway. What further
291 strengthens this hypothesis is the observation that some of the neurons, observed to be excited in relation
292 to seizures, showed significant phase coupling to the hippocampal LFP during the seizure.

293 The mechanism via which a majority of neurons are inhibited, on the other hand, may be a result of auto- or
294 hetero-inhibition. LC neurons are known to presynaptically express inhibitory α_2-adrenoceptors as
295 autoreceptors, both presynaptically at the axon terminals, but also on the cell bodies and dendrites (Berridge

296 & Waterhouse, 2003). LC neurons influence the activity of surrounding LC neurons through somatic and
297 dendritic release of noradrenaline (Andrade & Aghajanian, 1984; Huang et al., 2012). Strong excitation of a
298 subset of neurons, as observed in the present study, may thus result in inhibition of surrounding LC neurons.

299 The key takeaway from this study, with potentially strong clinical implications, is that evoked hippocampal
300 seizures in rodents consistently result in profound release of noradrenaline during seizures. Importantly, we
301 provide evidence of this not only in anesthetized rats, but also in freely moving awake rats. Although, at
302 present the extent to which the observed phenomenon is generalizable to other types of seizures is unknown,
303 there are a number of observations that could indicate that a profound release of noradrenaline is at least a
304 generalizable mechanism of limbic seizures. For example, we previously observed that evoking a status
305 epilepticus by infusing pilocarpine into the hippocampus in awake rats led to a strong increase in
306 concentrations of noradrenaline in the hippocampal extracellular space, measured with microdialysis (Raedt
307 et al., 2011). Another study showed that limbic seizures, evoked by electrical stimulation of the amygdala,
308 resulted in an increase in LC multiunit activity in awake rats and increased levels of noradrenaline in the LC
309 and amygdala. Silveira *et al.* further published a series of studies showing increased cFos expression in LC
310 neurons following acute limbic seizures in rats evoked with amygdala kindling, kainic acid or flurothyl (Silveira
311 et al., 2000, 2002; Silveira, Liu, de LaCalle, et al., 1998; Silveira, Liu, Holmes, et al., 1998). Further studies
312 should address the extent to which e.g. neocortical seizures and partial vs. generalized seizures similarly
313 modulate LC-noradrenergic transmission.

314 Noradrenaline is a powerful neuromodulator with profound effects on a number of physiological (and
315 pathophysiological) processes. Considering that the study at hand shows a consistent and profound release
316 of noradrenaline during hippocampal evoked seizures, addressing the physiological and/or
317 pathophysiological implications of this response may be necessary to understand the pathophysiology of
318 seizures. One of the most straight forward deductions is the role of noradrenaline in modulating arousal and
319 behavioral states (Berridge & Waterhouse, 2003). In general, levels of noradrenaline are thought to correlate
320 to levels of alertness. It is therefore puzzling that limbic seizures typically are associated with impairment or

321 even loss of consciousness (Englot et al., 2010). While we indeed consistently saw an increased release of
322 noradrenaline in the hippocampus, it is very possible that noradrenergic transmission decreases in other
323 areas relevant to consciousness (Gummadavelli et al., 2015) or that other mechanisms than release of
324 noradrenaline in relation to seizure mediate impaired consciousness associated with limbic seizures.

325 Noradrenaline is further known to affect physiology relevant to seizures, such as excitability and plasticity.
326 Although noradrenaline is predominantly seen as an anticonvulsant neuromodulator (Ghasemi &
327 Mehranfard, 2018), this is typically observed under conditions that involve a low-moderate facilitation of LC
328 activity and is predominantly (Corcoran & Weiss, 1990a) associated with activation of α-adrenoceptors,
329 which have relatively higher affinity of noradrenaline than β-adrenoceptors (Atzori et al., 2016). High levels
330 of noradrenaline, which may to a larger extent activate β-adrenoceptors has been associated with enhanced
331 excitability in hippocampal circuits (Harley & Milway, 1986; Heginbotham & Dunwiddie, 1991) and a mixture
332 of both anti- and pro-convulsant effects in rodent seizure models (Ghasemi & Mehranfard, 2018). The
333 question thus remains whether release of high levels of noradrenaline in relation to seizures protect against
334 or facilitate seizure activity.

335 Beyond immediate effects of noradrenaline on excitability, release of noradrenaline is known to enhance
336 plasticity, similarly through activation of β-adrenoceptors. For example, when high frequency stimulation is
337 paired with noradrenaline, induction of long-term potentiation (LTP) is enhanced (Hansen & Manahan-
338 Vaughan, 2015). Similarly, the consolidation of fear conditioning (Seo et al., 2021) or spatial memory (Hansen
339 & Manahan-Vaughan, 2015) is enhanced when paired with noradrenaline release. A consequence of
340 noradrenaline release in relation of seizure activity may be enhanced consolidation of pathological seizure
341 activity and facilitated formation of seizure networks, which could play a role in epileptogenesis. This
342 hypothesis has partially been studied in previous kindling experiments, by applying lesions to the LC-
343 noradrenergic system (Corcoran & Weiss, 1990). Such lesions, however, are associated with near complete
344 and chronic depletions of noradrenaline in the brain, which strongly exacerbates baseline seizure
345 severity (Giorgi et al., 2003), which severely complicates the interpretation of kindling experiments.

346 Addressing the role of noradrenaline released in relation to seizures will instead require tools that allow LC
347 specific modulation with high temporal precision and with sufficient potency to counter the strong excitatory
348 input to the LC during seizures.

349 In this study, we demonstrate that acute electrically evoked hippocampal seizures are associated with strong
350 changes in LC unit activity and strong and consistent time-locked release of noradrenaline. Understanding
351 the role of mass release of noradrenaline during hippocampal seizures is likely to be important to understand
352 seizure pathophysiology.

353 ## Materials and methods

354 All experiments were conducted with male Sprague Dawley rats (Envigo, The Netherlands, 300-400g at the
355 time of the experiment). Animals were treated according to European guidelines (directive 2010/63/EU). All
356 experiments described in the following were approved by the Animal Experimental Ethical Committee of
357 Ghent University (ECD 19/42 and 22/54). Rats were housed under environmentally controlled conditions
358 (humidity: 40-60%, temperature: 20-23°C), a controlled 12/12h light/dark cycle and food (Rats and Mice
359 Maintenance, Carfil, Belgium) and water *ad libitum*.

360 **Injection of viral vector in LC**

361 Prior to subsequent experimentation, 6 out of 14 rats used for LC unit recordings were injected in the LC with
362 a viral vector for LC specific expression of the blue-light gated chloride channel GtACR2 (**supplementary**
363 **Figure 2**). Injection of a CAV2 viral vector preceded acute LC unit recordings by at least 3 weeks. Rats were
364 anaesthetized using a mixture of isoflurane (5% for induction/2% for maintenance, Isoflo, Zoetis, UK) and
365 medical oxygen and fixed in a stereotactic frame. Bregma was lowered 2 mm relative to lambda to inject at
366 an angle of approximately 15 degrees, to avoid the transverse sinus. The LC was subsequently targeted
367 bilaterally with stereotactic coordinates 3.9 mm posterior and 1.2 mm lateral to lambda. At 3 depths, -5.5, -
368 5.8 and -6.1 mm relative to the brain surface, 0.6 µL of the viral vector construct CAV2-PRS-GtACR2-fRED
369 (titer 0.56×10^{12} pp/mL, IGMM, France) was injected at a rate of 100 nl/min, using a 5 µL Hamilton Neuros
370 Syringe (33 gauge, point style 3, Hamilton company, USA) and a Quintessential Stereotaxic Injection System
371 (Stoelting, USA). Following each injection, the needle was left in place for 5 minutes to prevent backflow of
372 the vector. At the end of the procedure, animals were injected with Meloxicam (1 mg/kg, Boehringer
373 Ingelheim, Germany) and left to recover for at least 3 weeks to allow expression of GtACR2.

374 **LC unit recordings and evoking of hippocampal seizures**

375 Acute LC unit recordings were performed in rats under isoflurane anesthesia (5% for induction/2% for
376 maintenance). Before targeting the LC, a polyimide-coated stainless steel wire electrode (ø70 µm, California

377 Fine Wire, USA) was implanted in the hilus of the dentate gyrus in the left dorsal hippocampus (3.8 mm
378 posterior, 1.9 mm lateral relative to bregma, ~-3 mm ventral to brain surface) for registration of local field
379 potentials (LFPs). A custom-made bipolar electrode for stimulation, made from two twisted polyimide coated
380 stainless steel wires (ø110 µm, Science products, Germany), was implanted in the left perforant
381 path (3.9 mm lateral to lambda, ~-2.5 mm ventral to brain surface). Electrodes were adjusted to obtain
382 maximal amplitude of evoked potentials in response to 200-400 mA bipolar square wave pules (0.2 ms pulse
383 width) delivered to the perforant path. Once in place, these electrodes were sealed in place with dental
384 cement and bound to surrounding bone screws (ø 0.8 mm, Plastics One). An additional wired bone screw
385 placed in the right frontal bone was used for grounding and as a reference for all electrophysiological
386 recordings in these experiments.

387 The LC was subsequently targeted using three different electrode set-ups: 1) a single-channel tungsten
388 microelectrode (0.00800/200 µm shank diameter, recording impedance ≥1.5 MΩ, FHC, USA), (n=9 rats), 2) a
389 32-channel silicon probe, model A1x32-Poly3-10mm-50-177, recording impedance ≥1.0 MΩ, Neuronexus,
390 USA), (n=8 rats), 3) a 32-channel silicon probe (model A1x32-Poly3-10mm-25-177, recording impedance ≥1.0
391 MΩ, Neuronexus, USA) with a Ø100 µm optic fiber (0.39 NA, FT100EMT, Thorlabs, Germany) attached
392 terminating at the most proximal electrode (n=6 rats). LC recordings with the high-density silicon probes
393 were performed to increase the yield of neurons recorded and the validity of the spike sorting process, which
394 is easier when action potentials of single neurons can be recorded over multiple electrode contacts in close
395 proximity. The latter probe was used for LC recordings in rats injected with viral vector for expression of
396 GtACR2, to additionally confirm the identity of LC neurons.

397 The initial LC coordinates used were 3.9 mm posterior and 1.15 mm lateral to lambda at an angle of
398 15 degrees towards the front. LC activity was usually found 5.5-6.2 mm ventral to brain surface. To confirm
399 the identity of LC activity, different parameters were used: 1) slow, regular firing patterns (1-6 Hz), with broad
400 spike waveforms (~1 ms), 2) a burst response (10-15 Hz) followed by inhibition (300-700 ms) upon application
401 of a noxious foot pinch (Vazey et al., 2018) and 3) optogenetic identification of LC activity. For subsequent

402 offline identification of LC activity, multiple trials of noxious foot pinch stimuli were performed (typically
403 around 10) separated by at least 30 seconds. For animals expressing GtACR2 in the LC, a number of light trials
404 (typically around 10) were performed for additional optogenetic confirmation of LC identity of the recorded
405 neurons. These trials, separated by at least 60 seconds, consisted of 3-7 second light pulses delivered at 4 mW
406 through the Ø100 µm optic fiber probe attached. Upon registration and stabilization of LC activity (typically
407 waited ~15 minutes), the experimental protocol was initiated.

408 Subsequently, a number of hippocampal seizures were evoked with 10 second tetanic trains of electrical
409 stimulation (20 Hz, 0.2 ms bipolar square wave pulses, DS4 Bi-Phasic Stimulator, Digitimer, USA). The
410 intensity was gradually increased until a reliable >10 s seizure was evoked in the hippocampal field (typically
411 at an intensity of 300-600 µA). Seizures were separated by at least 10 minutes. The number of seizures
412 evoked varied among animals (minimum was two, maximum was 10) depending on the stability of the LC
413 unit recordings. Recordings, except those including optogenetics, were concluded with an intraperitoneal
414 injection of the α_2-adrenoceptor agonist clonidine (0.04 mg/kg), to identify noradrenergic neurons that
415 respond with pronounced inhibition or silencing to the injection(Svensson et al., 1975).

416 **$GRAB_{NE2m}$ photometry experiments**

417 In a sequential experiment, changes in hippocampal noradrenergic transmission, during acute hippocampal
418 seizures, were assessed in 19 Sprague-Dawley rats using the $GRAB_{NE2m}$ fluorescent biosensor for
419 noradrenaline (Feng et al., 2019b). The $GRAB_{NE2m}$ sensor is a modified α_2-adrenoceptor with green
420 fluorescence protein (GFP) domain which increases its brightness upon binding of NA. Expression of the
421 $GRAB_{NE2m}$ sensor was induced in hippocampal neurons through injection of 600 nl of the viral vector construct
422 AAV9-hSyn-NE2m-mRuby3 (titer 10^{13} pp/mL, WZ Biosciences, USA) at 3.8 mm posterior and 1.9 mm lateral
423 to bregma and at a depth of -3.0 mm relative to brain surface. After at least two weeks, allowing the $GRAB_{NE2m}$
424 sensor to express, acute experiments were performed under isoflurane anesthesia (5% induction, 2%
425 maintenance). A bipolar stainless steel wire electrode was implanted at the lambda anterior-posterior
426 coordinate and 3.9 mm lateral to lambda at a depth of ~-2.5-3.0 mm relative to brain surface for perforant

427 path stimulation. A bipolar stainless steel wire electrode was implanted at 5.3 mm posterior and 3.2 mm
428 lateral to bregma and ~3 mm ventral to brain surface for acquisition of hippocampal LFPs. $GRAB_{NE2m}$
429 fluorescence was assessed by means of a Ø200 µm optic fiber (0.39 NA, FT200EMT, Thorlabs, Germany) and
430 photometry using the PyPhotometry acquisition board with the time division setting at a 130 Hz sample rate
431 (Akam & Walton, 2019). This system was paired with a 470 nm LED (Doric, Canada), a filter cube (Minicube,
432 Doric, Canada) allowing separation of light used for excitation (470 nm) and emitted fluorescence (~550 nm),
433 and a Femtowatt Silicon Photoreceiver (Model 2151, Doric, Canada). As in previous experiments, seizures
434 were evoked by 10 second tetanic trains of electrical perforant path stimulation (20 Hz, 0.2 ms bipolar square
435 wave pulses) at an intensity of 300-600 µA, while continuously monitoring $GRAB_{NE2m}$ fluorescence. Seizures
436 were separated by at least 10 minutes. Ten out of 19 animals were implanted for chronic experimentation
437 and allowed to recover for awake experimentation. In these cases, at least a week after the acute experiment,

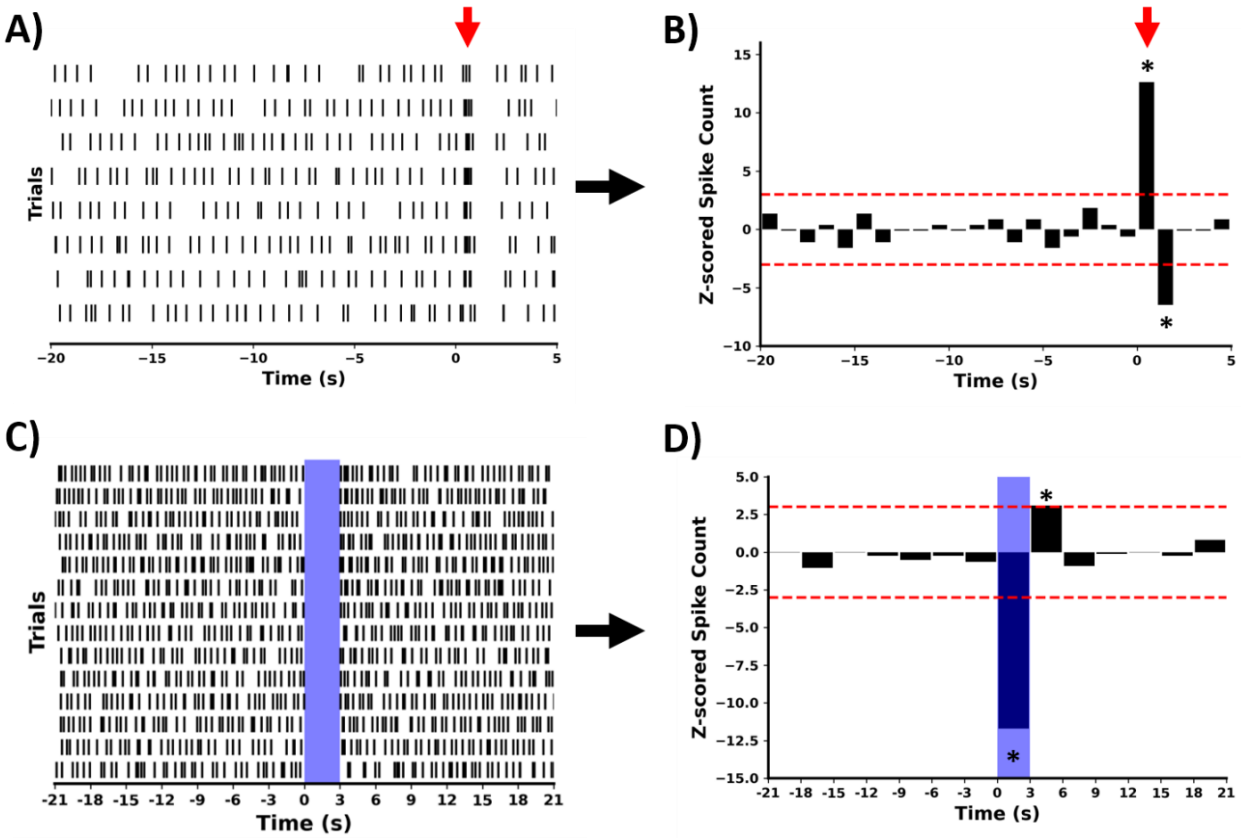

Figure 7: Identification of LC neurons on the basis of a response to a noxious mechanical foot pinch stimulus (A and B), or optogenetic tagging with GtACR2 (C and D). Trials were binned and averaged and a Z-score was calculated on the basis of the activity recorded before and after the application of the stimulus. A significant response to a noxious foot pinch or light (indicated with an asterisk here) was defined as a Z-score of ± 3 standard deviations (threshold indicated with horizontal dashed red lines). Application of the noxious mechanical foot pinch is indicated with a red arrow in A) and B), while blue light application in C) and D) is indicated with blue shading.

rats were attached to a custom-made electrophysiology-photometry setup allowing free movement via optical (Pigtailed fiber optic rotary joint, Doric, Canada) and electrical commutators. As under anaesthesia, seizures were evoked with 10 second tetanic trains of electrical perforant path stimulation (20 Hz, 0.2 ms bipolar square wave pulses) while recording hippocampal LFPs and $GRAB_{NE2m}$ fluorescence.

Electrophysiology hardware settings

Hippocampal LFPs were filtered and amplified (1-1000 Hz, 100x or 200x amplification) and digitized at 2 kHz with a 16 bit resolution over a ±10V input range using a National Instruments data acquisition device (National Instruments, Austin Texas, USA). LC unit activity acquired with a single channel tungsten needle

446 electrode was filtered and amplified (300-3000 Hz, 10000x amplification) and digitized at 30 kHz with a 16 bit
447 resolution over a ±10V input range using acquisition hardware (Micro1401-4) from Cambridge Electronic
448 Design (Cambridge, UK). LC unit activity acquired using a 32-channel silicon probe from Neuronexus was
449 analog filtered (1-7000 Hz) and digitized at 30 kHz with a 16 bit resolution over an effective ±6.4 mV input
450 range using Intan amplifier boards (Intan Technologies, Los Angeles, California, USA). Data acquisition was
451 done using an Open Ephys acquisition board (www.open-ephys.org) and stored for offline analysis.

452 **Data analysis and statistical analysis**

453 All digital signal processing, analysis and visualization was performed offline using custom scripts or software
454 made in Python. Spike-sorting of single-channel LC spike-data was done using Spike2 (Cambridge Electronic
455 Design, Cambridge, UK). Spike sorting on the basis of multi-channel recordings was done using SpyKING-
456 Circus (version 1.06) (Yger et al., 2018). Manual curation and merging of isolated spike clusters was
457 performed using the Phy GUI, from which spike trains were extracted for the respective putative single
458 neurons.

459 *Identification of LC activity*

460 LC activity was identified in 9 out of 14 animals, on the basis of a well characterized burst-inhibition response
461 to noxious stimuli (foot pinches), with optogenetic tagging, where possible, or as a response to the α_2-
462 adrenoceptor agonist clonidine (0.04 mg/kg, I.P.). During post hoc analysis foot pinch trials were evaluated
463 by binning spike rates in 1 second bins followed by averaging all trials. Z-scored bins were then computed
464 based on mean and standard deviation of the baseline, defined as 20 seconds prior to stimulus application.
465 A significant burst-inhibition response to a noxious foot pinch was defined as an initial burst bin exceeding a
466 Z-score of 3 ($p<0.01$), followed by an inhibition bin of less than -3 ($p<0.01$; for example, see **Figure 7A and B**).
467 Light trials were binned using a bin size equal to the duration of the light stimulus (3-7 seconds), followed by
468 averaging of trials. Z-scoring was done based on the mean and standard deviation of all bins around the light
469 stimulus (for example, see **Figure 7C and D**).

470 *Evaluation of LC neuronal activity during hippocampal seizures*

471 The activity of identified LC neurons during evoked hippocampal seizures was evaluated by initially
472 computing the spike rate in 5 second bins followed by Z-scoring derived from the mean and standard
473 deviation of the 300 seconds preceding the evoked seizure. In two cases, both within the same recording,
474 the evoked seizures did not last for 10 seconds and these seizures were thus excluded from further analysis.
475 A significant response to seizures was defined as a deviation of more than 1.96 standard deviations ($p<0.05$).
476 The consistency of responses of LC neurons over consecutive seizures was evaluated using Pearson
477 correlation analysis.

478 *Characteristics of LC neurons*

479 Characteristics of LC neurons were evaluated by three metrics: average spike rate, median interspike interval
480 and waveform asymmetry. The average spike rate and median spike interval were computed using data from
481 the entire recording, excluding a 60 second period around evoked seizures and excluding any period post
482 clonidine injection. Over the same period, the spike waveforms of the neurons were extracted from the
483 electrode contact where the neuron displayed the highest amplitude. Waveform asymmetry was computed
484 as an index of the amplitude of the two positive peaks of the spike waveforms as suggested by Totah *et*
485 *al.* (Totah et al., 2018a).

486 To look at cross-correlation of neurons in the period between seizures (inter-ictal activity), spikes from the
487 same time-frame between seizures were selected. Two types of cross-correlation common to LC neurons
488 were assessed as described by Totah *et al.* (Totah et al., 2018a). A 'sharp' type of coupling, hypothesized to
489 reflect electrotonic coupling of neurons, was calculated over a window of ±3 ms with a bin size of 0.5 ms. A
490 'broad' type of coupling, hypothesized to reflect putative common synaptic inputs, was calculated over a
491 window of ±200 ms with a bin size of 10 ms. For statistics, 200 jittered surrogate cross-correlograms were
492 computed per spike pair by jittering the spikes with ±1 ms (sharp coupling) or ±200 ms (broad coupling). Two
493 significant thresholds were computed: 1) a local 'per-bin' threshold computed from the mean ±3 standard

494 deviation of the jittered cross-correlograms, and 2) a global 'per cross-correlogram' threshold calculated as
495 the 99% minimum and maximum at any points of the computed jittered cross-correlograms. Cross-
496 correlograms with bins exceeding both of these thresholds were considered 'significant'. Rates of significant
497 cross-correlograms between conditions were compared in Fisher's exact tests.

498 *Topographies of multiunit activity*

499 The topography of multiunit activity, was computed by extracting threshold crossings per electrode contact
500 from the 32-channel silicon probe recordings. Threshold crossings were extracted using
501 SpyKINGCircus (v. 1.06) using a threshold of 7 median absolute deviations from the median of the signals.
502 Per contact, spike rates were binned (1 second bins) and Z-scored based on the mean and standard deviation
503 of firing. Significance was inferred for Z-scores higher or lower than 3 ($p<0.01$). Topography maps were
504 smoothed using cubic interpolation for graphical representation.

505 *Analysis of coupling of LC neuron activity to the hippocampal local field potential in relation to evoked seizures*

506 Temporal association between changes in firing of LC neurons and changes in the hippocampal LFP amplitude
507 were assessed using 50 seconds of data immediately following perforant path stimulation. Hippocampal LFP
508 'total' amplitude was calculated using the Fast Fourier Transform and binning per second. The spike rate of
509 LC neurons was similarly binned per second and cross-correlated with the hippocampal LFP amplitude to
510 assess peak cross-correlation indices. The peak cross-correlation and lag at peak cross-correlation was used
511 for a density-based cluster analysis to separate classes of neurons which subsequently were compared based
512 on the absolute peak cross-correlation and lag at peak cross-correlation using t-tests.

513 Coupling of LC neurons to the phase of frequency components of the hippocampal LFP, was computed using
514 exponentially scaling zero-phase second order bandpass filters (bands: 1-2 Hz, 4-8 Hz, 8-16 Hz, 16-32 Hz, 32-
515 64 Hz). The instant phase angles of the filtered hippocampal LFP were computed using the Hilbert Transform.
516 The phase angle probabilities of individual LC neurons were statistically assessed using circular statistics by

517 comparing the phase angle distribution to a uniform distribution, using a Rayleight test. Computed p-values
518 were adjusted for multiple comparison using Bonferroni correction.

519 Similarly, putative coupling of LC spikes to spikes in the hippocampal LFP was assessed. Negative spikes were
520 detected in the hippocampal LFP using a zero-phase highpass filter with a cutoff at 200 Hz followed by the
521 find_peaks function in the Python scipy.signal module. The LC spike count distribution around population
522 spikes was then calculated for a 1-second window around the population spikes and compared to a uniform
523 distribution using a Kolmogorov-Smirnov Test. Computed p-values were adjusted for multiple comparison
524 using Bonferroni correction.

525 *Analysis of $GRAB_{NE2m}$ fluorescence data*

526 Photometric data of $GRAB_{NE2m}$ fluorescence acquired in relation to evoked hippocampal seizures was
527 subjected to zero-phase low-pass filtering (cut-off at 1 Hz). The data was subsequently z-scored to the 300
528 seconds period before seizure induction. Significant changes in $GRAB_{NE2m}$ fluorescence were defined as
529 changes of at least 1.96 standard deviations ($p<0.05$) from pre-seizure levels. We further assessed changes
530 in fluorescence using the $\Delta F/F_0$ metric, which were then used to assess changes in fluorescence at a group
531 level using a one-sample t-test. Changes in $GRAB_{NE2m}$ fluorescence were additionally correlated to changes in
532 hippocampal LFP amplitude using one-second bins and cross-correlation.

533 **Histology**

534 Immediately following all acute recordings, animals were euthanized with an overdose of sodium
535 pentobarbital (Dolethal, 200 mg/kg, intraperitoneal, Vetoquinol, UK), followed by transcardial perfusion with
536 phosphate buffered saline (PBS) and paraformaldehyde (4%, pH 7.4). The brains were isolated from the skull,
537 post-fixed in 4% paraformaldehyde for 24h and cryoprotected for 3-4 days in a sucrose solution of 30% at
538 4°C. Subsequently the brains were snap-frozen in isopentane cooled in liquid nitrogen. Coronal sections of
539 40 µm were made using a cryostat (Leica, Germany). For immunohistochemistry, in order to visualize GtACR2
540 or $GRAB_{NE2m}$ expression, free floating slices were initially rinsed in distilled water, then incubated in 0.5%

541 H_2O_2 for 30 min and in 1% H_2O_2 for 60 min, to block endogenous peroxidase activity. Subsequently the
542 sections were washed in PBS (2x 5 min) and incubated in blocking buffer (BB, PBS containing 0.4% Fish Skin
543 Gelatin and 0.2% Triton X) for 45 min to block non-specific antibody binding sites. Sections were then
544 incubated with primary antibody diluted in BB for 1h at room temperature and overnight at 4°C. Mouse anti-
545 dopamine β-hydroxylase (DBH, 1:1000, Merck) was used to visualize LC neurons and rabbit anti-red
546 fluorescent protein to visualise the fRed tag (tRFP, 1:1000, Evrogen). For visualisation of $GRAB_{NE2m}$ expression
547 in the hippocampus, chicken anti-GFP (1:2000, Abcam) was used. A negative control containing BB without
548 antibodies was used. The following day, sections were rinsed in blocking buffer (2x 10 min) and incubated
549 with secondary antibodies: Alexa Fluor 488 goat anti-mouse (1:1000, Abcam), Alexa Fluor 594 goat anti-rabbit
550 (1:1000, Abcam) and Alexa Fluor 488 goat anti-chicken (1:1000, Abcam) diluted in BB for 1h at room
551 temperature in darkness. After rinsing in PBS (2x 5min), sections were mounted on glass slides and cover
552 slipped with Vectashield H1000 mounting medium (Vector Laboratories, USA) to prevent photo bleaching.

Acknowledgements

The research performed was supported by research grants from the Flemish Research Foundation (11M6422N) and the Queen Elisabeth Medical Foundation.

References

Akam, T., & Walton, M. E. (2019). pyPhotometry: Open source Python based hardware and software for fiber photometry data acquisition. *Scientific Reports 2019 9:1*, *9*(1), 1–11. https://doi.org/10.1038/s41598-019-39724-y

Andrade, R., & Aghajanian, G. K. (1984). Intrinsic regulation of locus coeruleus neurons: electrophysiological evidence indicating a predominant role for autoinhibition. *Brain Research*, *310*(2), 401–406. https://doi.org/10.1016/0006-8993(84)90170-7

Atzori, M., Cuevas-Olguin, R., Esquivel-Rendon, E., Garcia-Oscos, F., Salgado-Delgado, R. C., Saderi, N., Miranda-Morales, M., Trevino, M., Pineda, J. C., & Salgado, H. (2016). Locus Ceruleus Norepinephrine Release: A Central Regulator of CNS Spatio-Temporal Activation? *Front Synaptic Neurosci*, *8*, 25. https://doi.org/10.3389/fnsyn.2016.00025

Batiuk, M. Y., Martirosyan, A., Wahis, J., de Vin, F., Marneffe, C., Kusserow, C., Koeppen, J., Viana, J. F., Oliveira, J. F., Voet, T., Ponting, C. P., Belgard, T. G., & Holt, M. G. (2020). Identification of region-specific astrocyte subtypes at single cell resolution. *Nat Commun*, *11*(1), 1220. https://doi.org/10.1038/s41467-019-14198-8

Benarroch, E. E. (2018). Locus coeruleus. In *Cell and Tissue Research* (Vol. 373, Issue 1, pp. 221–232). Springer Verlag. https://doi.org/10.1007/s00441-017-2649-1

Berridge, C. W., & Waterhouse, B. D. (2003). The locus coeruleus-noradrenergic system: modulation of behavioral state and state-dependent cognitive processes. *Brain Res Brain Res Rev*, *42*(1), 33–84. http://www.ncbi.nlm.nih.gov/pubmed/12668290

Breton-Provencher, V., Drummond, G. T., & Sur, M. (2021a). Locus Coeruleus Norepinephrine in Learned Behavior: Anatomical Modularity and Spatiotemporal Integration in Targets. *Frontiers in Neural Circuits*, *15*, 46. https://doi.org/10.3389/FNCIR.2021.638007/BIBTEX

Breton-Provencher, V., Drummond, G. T., & Sur, M. (2021b). Locus Coeruleus Norepinephrine in Learned Behavior: Anatomical Modularity and Spatiotemporal Integration in Targets. *Frontiers in Neural Circuits*, *15*, 46. https://doi.org/10.3389/FNCIR.2021.638007/BIBTEX

Chandler, D. J., Jensen, P., McCal, J. G., Pickering, A. E., Schwarz, L. A., & Totah, N. K. (2019). Redefining Noradrenergic Neuromodulation of Behavior: Impacts of a Modular Locus Coeruleus Architecture. *The Journal of Neuroscience : The Official Journal of the Society for Neuroscience*, *39*(42), 8239–8249. https://doi.org/10.1523/JNEUROSCI.1164-19.2019

Clinckers, R., Zgavc, T., Vermoesen, K., Meurs, A., Michotte, Y., & Smolders, I. (2010). Pharmacological and neurochemical characterization of the involvement of hippocampal adrenoreceptor subtypes in the

588 modulation of acute limbic seizures. *J Neurochem*, *115*(6), 1595–1607.
589 https://doi.org/10.1111/j.1471-4159.2010.07065.x
590 Corcoran, M. E., & Weiss, G. K. (1990a). Noradrenaline and kindling revisited. In *Kindling 4* (pp. 141–156).
591 Springer.
592 Corcoran, M. E., & Weiss, G. K. (1990b). *Noradrenaline and Kindling Revisited*. 141–156.
593 https://doi.org/10.1007/978-1-4684-5796-4_11
594 Englot, D. J., Yang, L., Hamid, H., Danielson, N., Bai, X., Marfeo, A., Yu, L., Gordon, A., Purcaro, M. J.,
595 Motelow, J. E., Agarwal, R., Ellens, D. J., Golomb, J. D., Shamy, M. C. F., Zhang, H., Carlson, C., Doyle,
596 W., Devinsky, O., Vives, K., … Blumenfeld, H. (2010). Impaired consciousness in temporal lobe seizures:
597 role of cortical slow activity. *Brain : A Journal of Neurology*, *133*(Pt 12), 3764–3777.
598 https://doi.org/10.1093/BRAIN/AWQ316
599 Feng, J., Zhang, C., Lischinsky, J. E., Jing, M., Zhou, J., Wang, H., Zhang, Y., Dong, A., Wu, Z., Wu, H., Chen,
600 W., Zhang, P., Zou, J., Hires, S. A., Zhu, J. J., Cui, G., Lin, D., Du, J., & Li, Y. (2019a). A Genetically
601 Encoded Fluorescent Sensor for Rapid and Specific In Vivo Detection of Norepinephrine. *Neuron*,
602 *102*(4), 745-761.e8. https://doi.org/10.1016/J.NEURON.2019.02.037
603 Feng, J., Zhang, C., Lischinsky, J. E., Jing, M., Zhou, J., Wang, H., Zhang, Y., Dong, A., Wu, Z., Wu, H., Chen,
604 W., Zhang, P., Zou, J., Hires, S. A., Zhu, J. J., Cui, G., Lin, D., Du, J., & Li, Y. (2019b). A Genetically
605 Encoded Fluorescent Sensor for Rapid and Specific In Vivo Detection of Norepinephrine. *Neuron*,
606 *102*(4), 745-761.e8. https://doi.org/10.1016/j.neuron.2019.02.037
607 Ghasemi, M., & Mehranfard, N. (2018). Mechanisms underlying anticonvulsant and proconvulsant actions
608 of norepinephrine. *Neuropharmacology*, *137*, 297–308.
609 https://doi.org/10.1016/j.neuropharm.2018.05.015
610 Giorgi, F. S., Ferrucci, M., Lazzeri, G., Pizzanelli, C., Lenzi, P., Alessandrl, M. G., Murri, L., & Fornai, F. (2003).
611 A damage to locus coeruleus neurons converts sporadic seizures into self-sustaining limbic status
612 epilepticus. *Eur J Neurosci*, *17*(12), 2593–2601. https://doi.org/2692 [pii]
613 Gummadavelli, A., Kundishora, A. J., Willie, J. T., Andrews, J. P., Gerrard, J. L., Spencer, D. D., & Blumenfeld,
614 H. (2015). Neurostimulation to improve level of consciousness in patients with epilepsy. *Neurosurgical*
615 *Focus*, *38*(6). https://doi.org/10.3171/2015.3.FOCUS1535
616 Hansen, N., & Manahan-Vaughan, D. (2015). Hippocampal long-term potentiation that is elicited by
617 perforant path stimulation or that occurs in conjunction with spatial learning is tightly controlled by
618 beta-adrenoreceptors and the locus coeruleus. *Hippocampus*, *25*(11), 1285–1298.
619 https://doi.org/10.1002/hipo.22436

Harley, C. W. (2007). Norepinephrine and the dentate gyrus. *Prog Brain Res*, *163*, 299–318. https://doi.org/S0079-6123(07)63018-0 [pii] 10.1016/S0079-6123(07)63018-0

Harley, C. W., & Milway, J. S. (1986). Glutamate ejection in the locus coeruleus enhances the perforant path-evoked population spike in the dentate gyrus. *Exp Brain Res*, *63*(1), 143–150. https://doi.org/10.1007/bf00235656

Heginbotham, L. R., & Dunwiddie, T. v. (1991). Long-term increases in the evoked population spike in the CA1 region of rat hippocampus induced by beta-adrenergic receptor activation. *J Neurosci*, *11*(8), 2519–2527. http://www.ncbi.nlm.nih.gov/pubmed/1678426

Huang, H. P., Zhu, F. P., Chen, X. W., Xu, Z. Q. D., Zhang, C. X., & Zhou, Z. (2012). Physiology of quantal norepinephrine release from somatodendritic sites of neurons in locus coeruleus. *Frontiers in Molecular Neuroscience*, *5*(MARCH). https://doi.org/10.3389/FNMOL.2012.00029

Jimenez-Rivera, C. A., & Weiss, G. K. (1989a). The effect of amygdala kindled seizures on locus coeruleus activity. *Brain Res Bull*, *22*(4), 751–758. https://doi.org/10.1016/0361-9230(89)90095-6

Jimenez-Rivera, C. A., & Weiss, G. K. (1989b). The effect of amygdala kindled seizures on locus coeruleus activity. *Brain Research Bulletin*, *22*(4), 751–758. https://doi.org/10.1016/0361-9230(89)90095-6

Lee, C., Lavoie, A., Liu, J., Chen, S. X., & Liu, B. H. (2020). Light Up the Brain: The Application of Optogenetics in Cell-Type Specific Dissection of Mouse Brain Circuits. In *Frontiers in Neural Circuits* (Vol. 14). Frontiers Media S.A. https://doi.org/10.3389/fncir.2020.00018

Lima, S. Q., Hromádka, T., Znamenskiy, P., & Zador, A. M. (2009). PINP: A new method of tagging neuronal populations for identification during in vivo electrophysiological recording. *PLoS ONE*, *4*(7). https://doi.org/10.1371/journal.pone.0006099

Li, Y., Hickey, L., Perrins, R., Werlen, E., Patel, A. A., Hirschberg, S., Jones, M. W., Salinas, S., Kremer, E. J., & Pickering, A. E. (2016). Retrograde optogenetic characterization of the pontospinal module of the locus coeruleus with a canine adenoviral vector. *Brain Research*, *1641*(Pt B), 274–290. https://doi.org/10.1016/J.BRAINRES.2016.02.023

Mason, S. T., & Fibiger, H. C. (1979). Regional topography within noradrenergic locus coeruleus as revealed by retrograde transport of horseradish peroxidase. *The Journal of Comparative Neurology*, *187*(4), 703–724. https://doi.org/10.1002/CNE.901870405

McIntyre, D. C., Saari, M., & Pappas, B. A. (1979). Potentiation of amygdala kindling in adult or infants rats by injections of 6-hydroxydopamine. *Experimental Neurology*, *63*(3), 527–544. https://doi.org/10.1016/0014-4886(79)90169-9

Mishira, P. K., Burger, R. L., Bettendorf, A. F., Browning, R. A., & Jobe, P. C. (1994). Role of norepinephrine in forebrain and brainstem seizures: chemical lesioning of locus ceruleus with DSP4. *Experimental Neurology*, *125*(1), 58–64. https://doi.org/10.1006/EXNR.1994.1006

Raedt, R., Clinckers, R., Mollet, L., Vonck, K., el Tahry, R., Wyckhuys, T., de Herdt, V., Carrette, E., Wadman, W., Michotte, Y., Smolders, I., Boon, P., & Meurs, A. (2011). Increased hippocampal noradrenaline is a biomarker for efficacy of vagus nerve stimulation in a limbic seizure model. *J Neurochem*, *117*(3), 461–469. http://www.ncbi.nlm.nih.gov/pubmed/21323924

Sara, S. J. (2009). The locus coeruleus and noradrenergic modulation of cognition. *Nat Rev Neurosci*, *10*(3), 211–223. http://www.ncbi.nlm.nih.gov/pubmed/19190638

Sara, S. J., & Bouret, S. (2012). Orienting and Reorienting: The Locus Coeruleus Mediates Cognition through Arousal. *Neuron*, *76*(1), 130–141. http://www.ncbi.nlm.nih.gov/pubmed/23040811

Seo, D. oh, Zhang, E. T., Piantadosi, S. C., Marcus, D. J., Motard, L. E., Kan, B. K., Gomez, A. M., Nguyen, T. K., Xia, L., & Bruchas, M. R. (2021). A locus coeruleus to dentate gyrus noradrenergic circuit modulates aversive contextual processing. *Neuron*, *109*(13), 2116-2130.e6. https://doi.org/10.1016/J.NEURON.2021.05.006

Silveira, D. C., Liu, Z., de LaCalle, S., Lu, J., Klein, P., Holmes, G. L., & Herzog, A. G. (1998a). Activation of the locus coeruleus after amygdaloid kindling. *Epilepsia*, *39*(12), 1261–1264. http://www.ncbi.nlm.nih.gov/pubmed/9860060

Silveira, D. C., Liu, Z., de LaCalle, S., Lu, J., Klein, P., Holmes, G. L., & Herzog, A. G. (1998b). Activation of the locus coeruleus after amygdaloid kindling. *Epilepsia*, *39*(12), 1261–1264. https://doi.org/10.1111/J.1528-1157.1998.TB01323.X

Silveira, D. C., Liu, Z., Holmes, G. L., Schomer, D. L., & Schachter, S. C. (1998a). Seizures in rats treated with kainic acid induce Fos-like immunoreactivity in locus coeruleus. *Neuroreport*, *9*(7), 1353–1357. http://www.ncbi.nlm.nih.gov/pubmed/9631428

Silveira, D. C., Liu, Z., Holmes, G. L., Schomer, D. L., & Schachter, S. C. (1998b). Seizures in rats treated with kainic acid induce Fos-like immunoreactivity in locus coeruleus. *Neuroreport*, *9*(7), 1353–1357. https://doi.org/10.1097/00001756-199805110-00019

Silveira, D. C., Schachter, S. C., Schomer, D. L., & Holmes, G. L. (2000). Flurothyl-induced seizures in rats activate Fos in brainstem catecholaminergic neurons. *Epilepsy Res*, *39*(1), 1–12. https://doi.org/S0920-1211(99)00106-0 [pii]

Silveira, D. C., Sogawa, Y., & Holmes, G. L. (2002). The expression of Fos following kainic acid-induced seizures is age-dependent. *Eur J Neurosci*, *15*(2), 329–344. https://doi.org/1849 [pii]

Svensson, T. H., Bunney, B. S., & Aghajanian, G. K. (1975). Inhibition of both noradrenergic and serotonergic neurons in brain by the alpha-adrenergic agonist clonidine. *Brain Research*, *92*(2), 291–306. https://doi.org/10.1016/0006-8993(75)90276-0

Totah, N. K., Neves, R. M., Panzeri, S., Logothetis, N. K., & Eschenko, O. (2018a). The Locus Coeruleus Is a Complex and Differentiated Neuromodulatory System. *Neuron*, *99*(5), 1055-1068 e6. https://doi.org/10.1016/j.neuron.2018.07.037

Totah, N. K., Neves, R. M., Panzeri, S., Logothetis, N. K., & Eschenko, O. (2018b). The Locus Coeruleus Is a Complex and Differentiated Neuromodulatory System. *Neuron*, *99*(5), 1055-1068.e6. https://doi.org/10.1016/J.NEURON.2018.07.037

Uematsu, A., Tan, B. Z., Ycu, E. A., Cuevas, J. S., Koivumaa, J., Junyent, F., Kremer, E. J., Witten, I. B., Deisseroth, K., & Johansen, J. P. (2017). Modular organization of the brainstem noradrenaline system coordinates opposing learning states. *Nature Neuroscience*, *20*(11), 1602–1611. https://doi.org/10.1038/NN.4642

Vazey, E. M., Moorman, D. E., & Aston-Jones, G. (2018). Phasic locus coeruleus activity regulates cortical encoding of salience information. *Proceedings of the National Academy of Sciences of the United States of America*, *115*(40), E9439–E9448. https://doi.org/10.1073/PNAS.1803716115/SUPPL_FILE/PNAS.1803716115.SAPP.PDF

Vermoesen, K., Massie, A., Smolders, I., & Clinckers, R. (2012). The antidepressants citalopram and reboxetine reduce seizure frequency in rats with chronic epilepsy. *Epilepsia*, *53*(5), 870–878. https://doi.org/10.1111/j.1528-1167.2012.03436.x

Yger, P., Spampinato, G. L., Esposito, E., Lefebvre, B., Deny, S., Gardella, C., Stimberg, M., Jetter, F., Zeck, G., Picaud, S., Duebel, J., & Marre, O. (2018). A spike sorting toolbox for up to thousands of electrodes validated with ground truth recordings in vitro and in vivo. *Elife*, *7*. https://doi.org/10.7554/eLife.34518